Figure 2. Kanai *et al.*

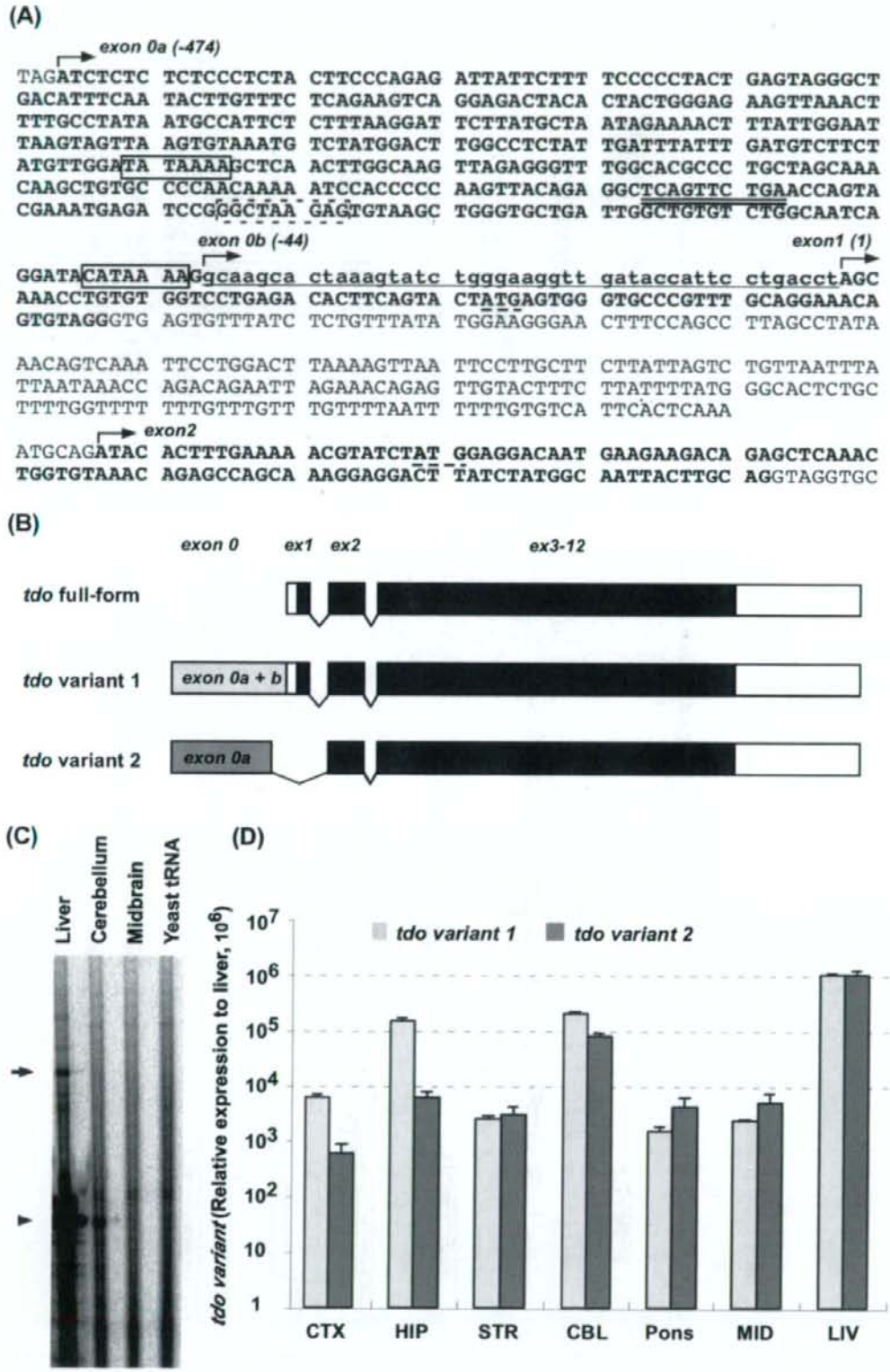

Figure 3. Kanai *et al*.

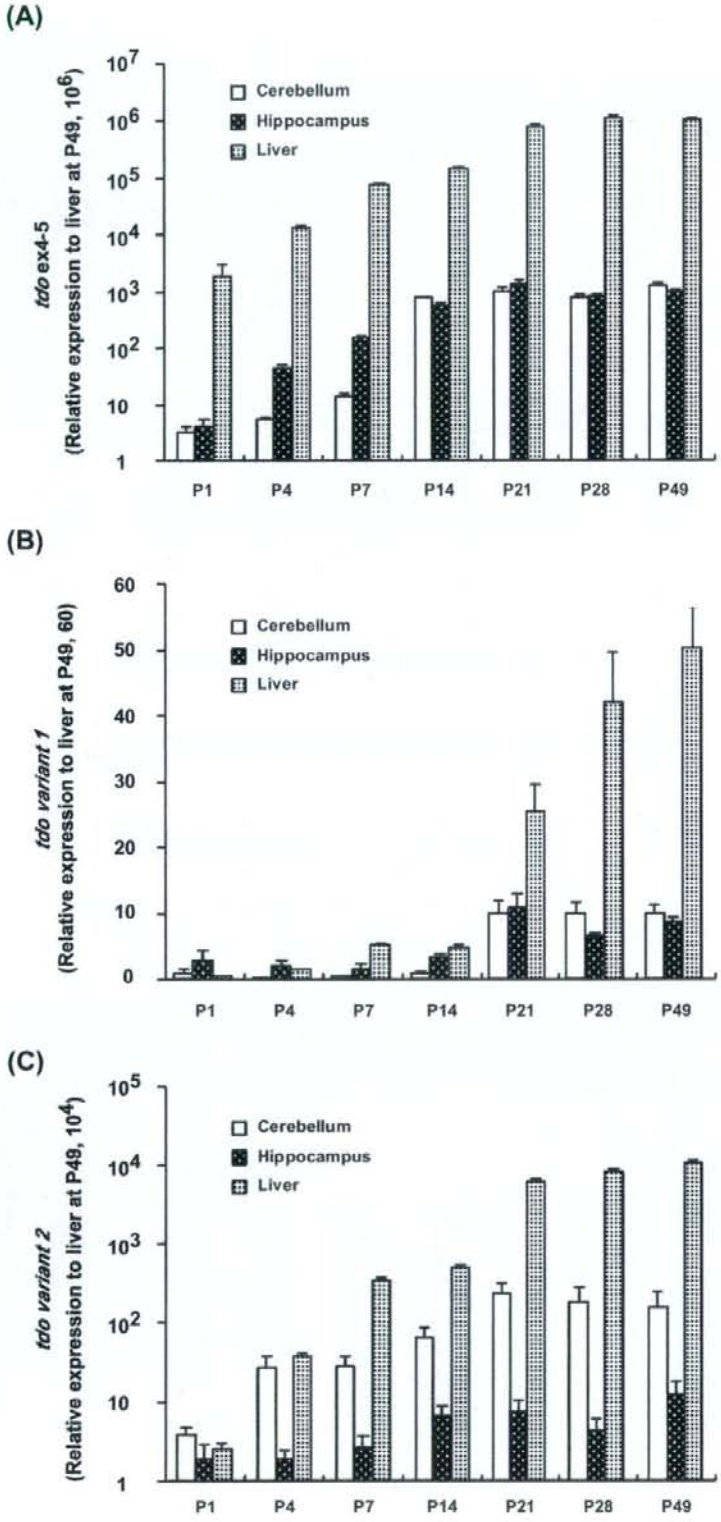

Figure 4. Kanai *et al.*

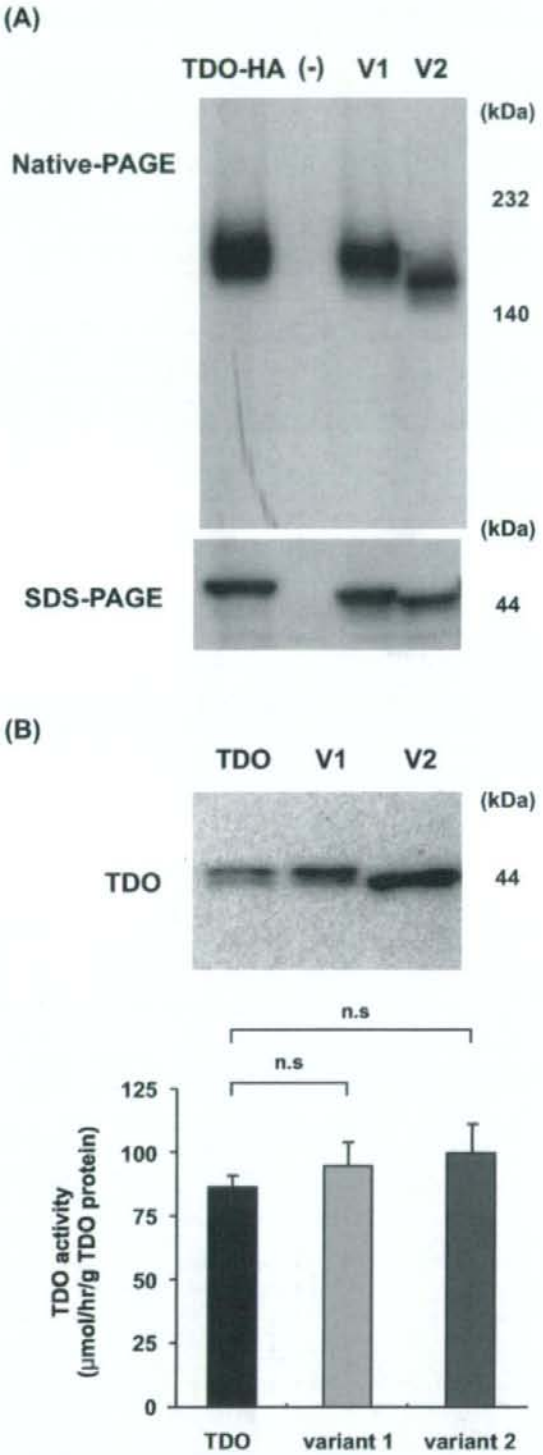

J Neuropathol Exp Neurol

Vol. 68, No. 1
January 2009
pp. 37–47

ORIGINAL ARTICLE

Nuclear TAR DNA Binding Protein 43 Expression in Spinal Cord Neurons Correlates With the Clinical Course in Amyotrophic Lateral Sclerosis

Hisae Sumi, MD, PhD, Shinsuke Kato, MD, PhD, Yuko Mochimaru, Harutoshi Fujimura, MD, PhD, Masaki Etoh, MD, PhD, and Saburo Sakoda, MD, PhD

Abstract

TAR DNA binding protein 43 (TDP-43) has been considered a signature protein in frontotemporal dementia and amyotrophic lateral sclerosis (ALS), but not in ALS associated with the superoxide dismutase 1 (*SOD1*) gene mutations (ALS1). To clarify how TDP may be involved in ALS pathogenesis, clinical and pathological features in cases of sporadic ALS ([SALS] n = 18) and ALS1 (n = 6) were analyzed. In SALS patients with rapid clinical courses, TDP mislocalization (i.e. cytoplasmic staining and TDP-positive cytoplasmic inclusions) in anterior horn cells was frequent. In SALS patients with slow clinical courses, TDP-43 mislocalization was rare. In an ALS1 patient with the *SOD1* gene mutation C111Y, there were numerous TDP-positive inclusions and colocalization of SOD1 and TDP. In mutant SOD1 transgenic (G93A) mice at the end stage (median, 256 days), TDP-positive inclusions and TDP colocalization with SOD1 were also observed; nuclear TDP-43 immunoreactivity was highly correlated with life span in these mice. In both humans and mice, nuclei that stained strongly for TDP were large and circular; weakly stained nuclei were atrophic or deformed. In conclusion, low levels of TDP expression in the nucleus cor relate with a rapid clinical course in SALS and in ALS1 model mice, suggesting that nuclear TDP may play a protective role against motor neuron death resulting from different underlying etiologies.

Key Words: Amyotrophic lateral sclerosis, ALS, Anterior horn cell, ALS1, G93A transgenic mice, Lewy body–like hyaline inclusion, SOD1, TDP-43.

INTRODUCTION

Amyotrophic lateral sclerosis (ALS) is a fatal motor neuron disease that causes progressive motor paralysis. The underlying pathogenetic mechanisms are largely unknown in 90% of ALS patients, that is, those with sporadic ALS (SALS). Of the 10% of ALS cases with familial ALS (FALS), approximately one fifth are associated with a mutation in the superoxide dismutase 1 (*SOD1*) gene; these patients are classified as ALS1 (1, 2). The pathogenesis of ALS1 is thought to involve aggregation of mutant SOD1 and subsequent oxidative stress (3). Another rare cause of juvenile autosomal recessive FALS is the gene that encodes ALS2, also known as alsin (4, 5). In most cases of FALS, however, the causative gene has not been identified because of low penetrance.

TAR DNA binding protein 43 (TDP-43), a nuclear protein, contains 2 fully functional RNA recognition motif domains and a C-terminal region that is capable of binding directly to several proteins of the heterogeneous nuclear ribonucleoprotein family (6–8); these ribonucleoproteins have a variety of functions including the modification, stabilization, and transport of RNA. The TDP modifies the splicing of exon 9 of the cystic fibrosis transmembrane conductance regulator gene (9) and of exon 3 of the apolipoprotein A-II gene (10). Recently, it also has been reported that loss of TDP in vitro results in nuclear dysmorphism, misregulation of the cell cycle, and apoptosis (11).

Neuronal inclusions, such as Lewy body–like hyaline inclusions (LBHIs), or the aggregation of mutant SOD1 in ALS1 (3, 12) are known to be important pathological features in the pathogenesis of neurodegenerative diseases. The TDP is a component of the ubiquitin-positive inclusions and neurites observed in frontotemporal dementia and ALS (13, 14). The TDP-positive round or filamentous inclusions in the cytoplasm and mislocalization of TDP from the nucleus to the cytoplasm have been observed in all cases of SALS (15) and FALS, but not in ALS1 (16, 17). A novel missense mutation in TDP was recently identified as causative in familial motor neuron disease and SALS (18, 19). Although the concept of TDP proteinopathy has been suggested (14, 20), the presence of TDP-positive inclusions in other diseases, including hippocampal sclerosis, Alzheimer disease (21), Parkinson disease (22), Pick disease (23), and neoplastic lesions (24), complicates this issue. Furthermore, Sanelli et al (25) have reported that TDP is not a major ubiquitinated target within the pathological inclusions of ALS.

From the Department of Neurology, Osaka University Graduate School of Medicine (HS, ME, SS), Yamadaoka, Suita; Department of Neuropathology, Institute of Neurological Sciences, Faculty of Medicine, Tottori University (SK), Nishi-cho, Yonago; Department of Health Science, Osaka University Graduate School of Medicine (YM), Yamadaoka, Suita; and Department of Neurology, Toneyama National Hospital (HF), Toneyama, Toyonaka, Japan.

Send correspondence and reprint requests to: Hisae Sumi, MD, PhD, Department of Neurology, Osaka University Graduate School of Medicine, 2-2 Yamadaoka, Suita, 565-0871, Japan; E-mail: hasumi@neurol.med.osaka-u.ac.jp

This study was supported by the Health and Labor Sciences Research on Measures for Incurable Disease, Ministry on Health, Labor and Welfare of Japan.

TABLE. Clinical and Pathological Data*

Patients	Age, years	Disease Duration, years	Initial Weakness Manifestation	Use of Respirator (Estimated Duration)	Cause of Death	Family History	No. Large Neurons†	No. Large Neurons With TDP Mislocalization†	No. Neuronal Inclusions†	No. Glial Inclusions†
SALS r-1	69	0.7	L	No	Pneumonia	No	13	6 (I)	40	16
SALS r-2	77	0.8	U	No	Resp. f.	No	23	8 (I>D)	34	4
SALS r-3	49	0.8	L, B	No	Resp. f.	No	9	4 (I)	35	6
SALS r-4	60	1.5	B, U	No	Pneumonia	No	36	12 (D>I)	25	38
SALS r-5	59	1.5	U	No	Resp. f.	No	16	9 (D>I)	12	22
SALS r-6	69	2	B, U	No	Resp. f.	No	22	12 (D>I)	25	38
SALS r-7	51	2	B	No	Resp. f.	No	22	11 (D>I)	21	11
SALS r-8	71	2	U	No	Resp. f.	No	21	4 (I>D)	69	8
SALS r-9	61	2	U	No	Resp. f.	No	8	3 (I>D)	12	9
SALS r-10	64	2	L	No	Pneumonia	No	7	0	9	123
SALS r-11	73	2.5	B	No	Resp. f.	No	25	4 (I>D)	14	7
SALS r-12	60	2.5	B, U	No	Resp. f.	No	12	7 (D>I)	18	19
SALS r-13	71	2.5	U	No	Resp. f.	No	4	0	26	26
SALS s-1	79	5	U	No	Resp. f.	No	2	0	0	0
SALS s-2	53	5.5	U	No	Resp. f.	No	9	0	4	2
SALS s-3	63	5.5	U, L	No	Resp. f.	No	4	0	2	2
SALS s-4	48	6.7	?	No	Resp. f.	No	15	0	0	2
SALS s-5	45	7.3	?	No	Resp. f.	No	2	0	0	3
				Median (range), 62 (45–79); 2.0 (0.7–7.3)						
ALS1-1 (C111Y)	71	7	L	3 years	Ren f.	Yes	0	0	20	31
ALS1-2 (126 2bp del)	42	2	L	0.5 years	Pneumonia	Yes	3	1 (D)	0	0
ALS1-3 (126 2bp del)	65	11	L	10 years	Hemorrhage	Yes	0	0	0	0
ALS1-4 (G37R)	50	9	U	2.5 years	Pneumonia	Yes	1	0	0	0
ALS1-5 (L126S)	67	9	L	No	Resp. f.	Yes	13	0	0	0
ALS1-6 (L126S)	45	8.5	L	No	Resp. f.	Yes	7	0	0	0
				Median (range), 58 (42–71); 9 (2–11)						

*ALS1, amyotrophic lateral sclerosis (*SOD-1* gene mutation); B, bulbar; D, diffuse staining pattern; D > I, predominantly diffuse staining pattern; I, inclusion pattern; I > D, predominantly inclusion pattern; L, lower limb; Ren. f., renal failure; Resp. f., respiratory failure; SALS r, sporadic ALS with a rapid clinical course (i.e. ≤2.5 years); SALS s, SALS with a slow clinical course; U, upper limb.

†Large neurons with cytoplasm exceeding 37 μm in diameter and clear nucleoli were counted. TAR DNA binding protein (TDP) mislocalization includes a diffuse staining pattern in the cytoplasm (D) and TDP-positive inclusions in the cytoplasm (I). Cell types containing TDP-positive inclusions were estimated as neuronal or glial on the basis of the morphology of their nuclei and cytoplasm.

To clarify how TDP may be involved in pathogenetic mechanisms in ALS, we examined SALS and ALS1 patients clinically and pathologically by immunohistochemistry using an anti-TDP antibody. We also examined the lumbar spinal cords of mutant SOD1 transgenic mice (G93A mice) that have lower copy numbers of the mutant *SOD1* gene than the G93A mice previously examined by Robertson et al (26); G93A mice with low copy numbers of the mutant *SOD1* gene show pathological changes that are similar to those in patients with ALS (27).

MATERIALS AND METHODS

ALS Cases and Pathological Assessment

Fixed paraffin-embedded 4-μm-thick sections through the lumbar spinal cord at the L5 level were obtained from Osaka University Graduate School of Medicine (Suita) for clinicopathologic analysis. These patients had SALS (n = 18; age at death 62 [median, 45–79] years; disease duration, 2 [0.7–7.3] years) or ALS1 (n = 6; age at death, 58 [42–71] years; disease duration, 9 [2–11] years; Table). All neuropathologic analyses were performed by trained neuropathologists. Sporadic ALS patients who did and did not have a history of respirator use and whose deaths were caused by respiratory failure or pneumonia were examined. Clinical data including the localization of initial symptoms, history of respirator use, cause of death, and family history are shown in the Table.

Deparaffinized sections were incubated for 30 minutes with 0.3% hydrogen peroxide to quench endogenous peroxidase activity and then washed with PBS. The primary antibodies used were rabbit polyclonal antibodies against TDP-43 (1:3000, Protein Tech Group, Chicago, IL) and ubiquitin (1:2000, Dako, Glostrup, Denmark), mouse monoclonal antibodies against human SOD1 (0.5 μg/mL, clone 1G2, MBL, Aichi, Japan) and phosphorylated neurofilament (1:10,000, SMI31, Covance, Berkeley, CA), and a sheep polyclonal antibody against human SOD1 (1:20,000, Calbiochem, San Diego, CA); these were applied to serial sections as primary antibodies. Goat anti-rabbit and anti-mouse immunoglobulins conjugated to peroxidase-labeled dextran polymer (ready to use, Dako Envision+, Dako Corp, Carpinteria, CA) and rabbit anti-sheep immunoglobulin (1:1000, Abcam PLC, Cambridge, United Kingdom) were used as secondary antibodies. Reaction products were visualized with 3,3′-diaminobenzidine tetrahydrochloride (ImmPACT DAB, Vector Laboratories, Burlingame, CA), and hematoxylin was used to counterstain cell nuclei.

To estimate the numbers of TDP-positive cytoplasmic inclusions, large neurons that had clear nucleoli and cell bodies with a diameter greater than 37 μm (28) (presumed to be α motoneurons) and the numbers of neurons with TDP mislocalization from the nucleus to the cytoplasm in the gray matter, from video images of each section obtained with a digital camera (Keyence VB-7010, Keyence, Osaka) attached to a light microscope (EclipseE800, Nikon, Tokyo), were counted. The diameters of the neurons were measured with the aid of image analysis software (VH-H1A5, Keyence). Mislocalization of TDP was defined as the presence of a TDP-negative nucleus and TDP-positive cytoplasm. In mislocalizations of TDP, there can also be diffuse staining patterns in the cytoplasm and TDP-positive filamentous or round inclusions in the cytoplasm. Cells containing TDP-positive inclusions were classified as neurons or glia on the basis of the shape of their nuclei and cytoplasm.

Animals

Transgenic mice expressing the mutated human *SOD1* (G93A) gene at a low level (B6SJL-TgN[SOD1]-G93A)1Gur[dl] [G1L]) were obtained from Jackson Laboratory (Bar Harbor, ME). These mice carry 18 transgene copies because of a reduction in the copy number compared with (B6SJL-TgN[SOD1]-G93A)1Gur (G1H) mice, which express 25 copies (3). The G1L mice were bred and maintained as hemizygotes by mating with wild-type B6.SJL mice. Non-transgenic littermates were used as controls. All animals were genotyped and handled as previously described (29). We examined control (n = 6,292 [median, 240–296] days old) and G1L (n = 9,256 [224–281] days old, end stage) mice. One G1H mouse (120 days, end stage), also obtained from Jackson Laboratory, was examined to confirm the lack of TDP-43 abnormalities reported previously (26). *End stage* was defined as occurring when the mouse was so severely paralyzed that it could hardly move or drink water. The mice were killed with an overdose of sodium pentobarbital and perfused with PBS followed by 4% paraformaldehyde. The lumbar enlargement of the spinal cord was removed, immersed in 4% paraformaldehyde overnight at 4°C, and then dehydrated and embedded in paraffin blocks. Paraffin sections, 4-μm-thick, were prepared and stained with hematoxylin and eosin. Every fifth section (cut at 20-μm intervals) was obtained, and 4 sections from each mouse were used to count the total number of LBHIs in the sections. For immunohistochemistry, the primary antibodies used on the serial sections were against TDP-43 (1:600, Protein Tech Group) and human SOD1 (0.5 μg/mL, clone 1G2, MBL, Nagoya, Japan).

Semiquantitative Analysis of Immunoreactivity for TDP

Because variation in the TDP immunoreactivity (TDP-IR) was evident among G1L mice, the patterns of TDP immunostaining were divided into normal (0) and abnormal (1 to 4), the latter showing TDP-positive neurites and inclusions and varying degrees of nuclear positivity. The stages of normal or abnormal patterns were classified by TDP-IR of the neuron nuclei as follows: normal pattern (Stage 0): same as in normal littermates, with immunoreactivity apparent only in nuclei; abnormal pattern (Stages 1–4): Stage 1, weak immunoreactivity in nuclei; Stage 2, weak to moderate immunoreactivity in nuclei; Stage 3, moderate to strong immunoreactivity in nuclei; Stage 4, strong immunoreactivity in nuclei.

Quantitative Analysis of LBHIs

The numbers of LBHIs with a core and halo in neurons of the lumbar spinal cord were counted in hematoxylin and

eosin–stained sections (100× objective) from each G1L mouse as previously described (29).

Statistical Analysis

Differences in the numbers of TDP-positive inclusions in neurons and glia and in large neurons (>37 μm) between SALS patients with a rapid course and those with a slow course were analyzed by Wilcoxon rank sum test. The relationships among the numbers of large neurons and TDP-positive inclusions in neurons and glia were also analyzed using Spearman correlation coefficient with a 95% confidence interval (CI). In G1L mice, the relationships among age at the end stage, number of LBHIs, and TDP-IR were analyzed using Spearman correlation coefficient with 95% CI. Exploratory subgroup analyses for age at the end stage were done in the TDP-IR weak groups (Stages 1 and 2) and the TDP-IR strong groups (Stages 3 and 4) by Kolmogorov-Smirnov test. All statistical analyses were performed with SAS version 9.1 (SAS Institute Inc, Cary, NC).

RESULTS

ALS Cases

In the lumbar cords of SALS patients with disease durations less than or equal to 2.5 years (SALS r-1 to -13), mislocalization of TDP was frequently observed (Figs. 1B, C; Table); this was not evident in controls (Fig. 1A). There was a diffuse cytoplasmic staining pattern, especially in large neurons (>37 μm, Fig. 1B) and TDP-positive filamentous or round inclusions were evident in atrophic neurons and in glia (Figs. 1C, D); the nuclei in the neurons and glia were negative for TDP. In SALS patients with mild to moderate neuronal loss, there was often a diffuse TDP staining pattern in the cytoplasm of large neurons (Table). No extracellular TDP-positive inclusions were apparent. By contrast, in SALS patients with disease durations longer than 5 years (SALS s-1 to -5), neurons with diffuse cytoplasmic staining patterns were not evident, and TDP-positive inclusions were only rarely detected (Table). The TDP-IR of the nuclei of residual neurons appeared to be preserved.

In ALS1 patients, diffuse cytoplasmic TDP staining of large neurons was found only in 1 patient, i.e. ALS1-2 (126 2bp del), who had a clinical course of 2 years (Table). Some small neurons in Patients ALS1-2 and ALS1-3 (126 2bp del) also showed diffuse cytoplasmic TDP staining (Figs. 3A, C). The TDP-positive inclusions were prominent in the glia and in small neurons or their neurites in Patient ALS1-1 (C111Y), who had no remaining large neurons. The nuclei of cells with TDP-positive inclusions were TDP negative (Figs. 2A, E). Colocalization of TDP and SOD1 was frequently evident as

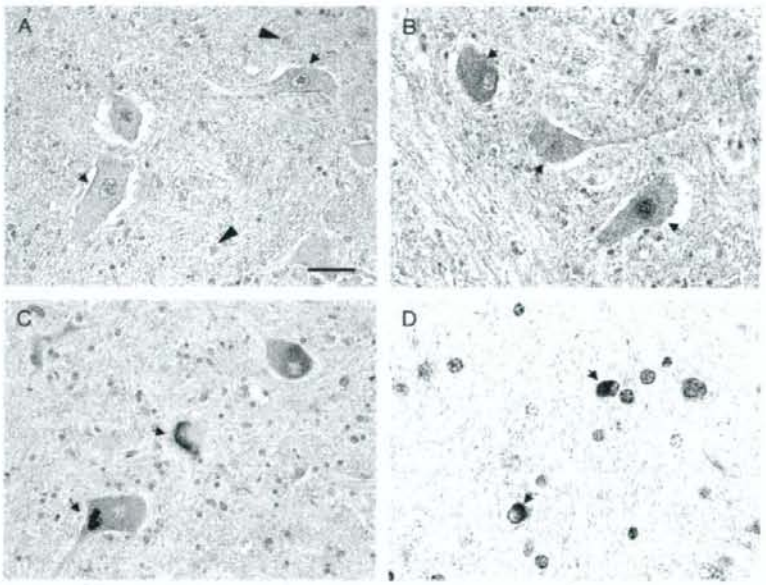

FIGURE 1. Mislocalization of TAR DNA binding protein (TDP) in cases of sporadic amyotrophic lateral sclerosis (SALS) with rapid clinical courses. **(A)** Normal control. The nuclei of large neurons are positive for TDP (arrows). Some glia (arrowheads) are weakly stained. **(B–D)** SALS patients. **(B)** There is diffuse punctate cytoplasmic staining in the neuron on the left (arrow), and heterogeneous staining in the middle (arrow) is observed in the cytoplasm. Nuclei of neurons on the left and in the middle are negative for TDP, whereas the nucleus of the neuron on the right is stained. **(C)** Variable appearances of cytoplasmic TDP inclusions (arrows). The structure on the left (arrow) is rounded, whereas the one in the middle neuron is elongated and filamentous (arrow). **(D)** Glial inclusions are positive for TDP (arrows). Immunohistochemistry against TDP. Scale bar = 50 μm.

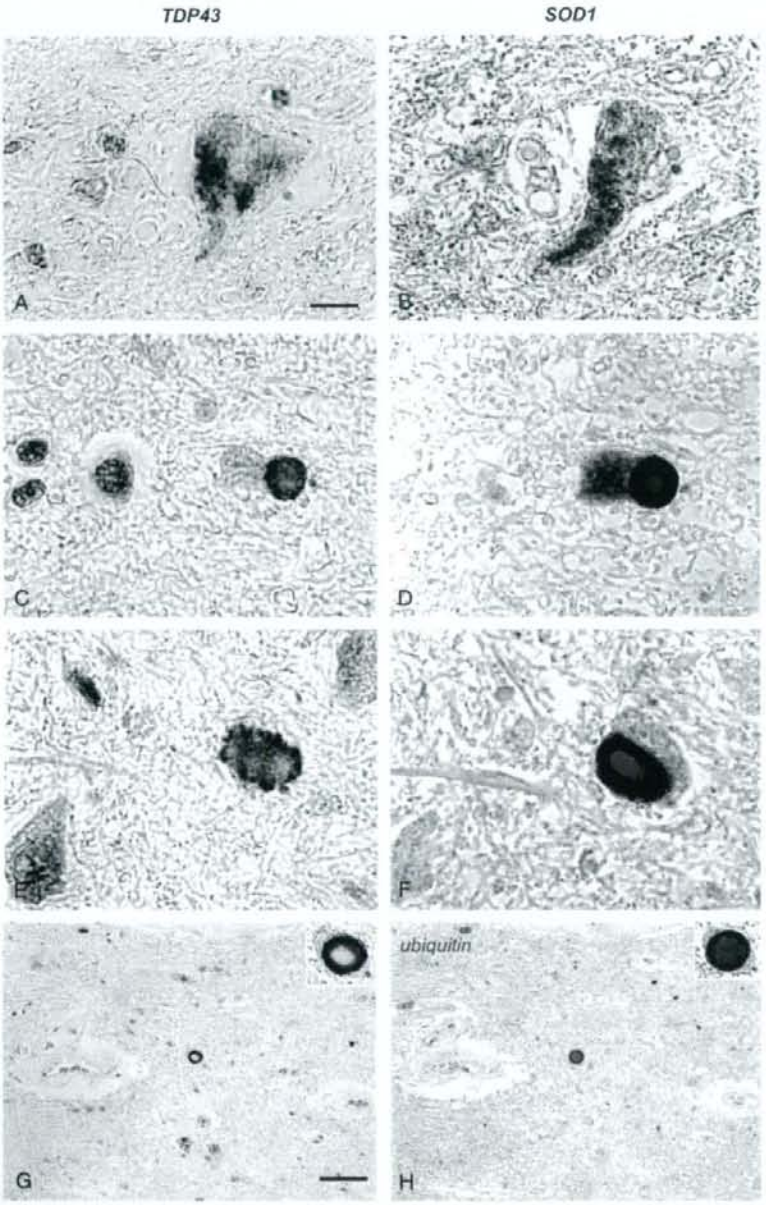

FIGURE 2. Colocalization of TAR DNA binding protein (TDP) and superoxide dismutase 1 (SOD1) in neurons of an amyotrophic lateral sclerosis 1 (C111Y) patient. **(A, B)** Heterogeneous cytoplasmic staining patterns for TDP **(A)** and for SOD1 **(B)**. The nucleus is TDP negative. **(C–F)** Neuronal inclusions are positive for TDP **(C, E)** and SOD1 **(D, F)**. **(G, H)** The halo portion of a Lewy body–like hyaline inclusion (LBHI) is stained strongly for TDP **(G)** and ubiquitin **(H)**. The upper panels are high-magnification views of each LBHI. Immunohistochemistry: **(A, C, E, G)** = TDP; **(B, D, F)** = SOD1; **(H)** = ubiquitin. **(B, D, F,** and **H)** are adjacent serial sections of **(A, C, E,** and **G)**, respectively. Scale bars = **(A–F)** 10 μm; **(G, H)** 50 μm; insets in **(G, H)** = 16 μm.

an aggregation pattern (Figs. 2A–F). The TDP and ubiquitin were also colocalized in inclusions (Figs. 2G, H). Patients ALS1-2 (30) and ALS1-3 (31) possessed the same SOD1 mutation; TDP-IR of the nuclei was weaker in Patient ALS1-3,who had more LBHIs than Patient ALS1-2. The TDP-IR of some of the LBHIs observed in these patients was weak, but stronger than that in most of the nuclei (Fig. 3A). Colocalization of TDP and SOD1 was demonstrated in LBHIs in serial sections (Figs. 3A, B). The LBHIs were scarce in other ALS1 patients. Although TDP-IR was retained in the nuclei of most of the residual neurons in Patients ALS1-4 (G37R) (32) and ALS1-5 (L126S) (33), there were a few neurons with TDP-negative nuclei and cytoplasm. The TDP-negative nuclei were atrophic or deformed (Fig. 3D), whereas most of the TDP-positive nuclei were circular (Fig. 3F). In ALS1 patients, there was no apparent relationship between nuclear TDP-IR and disease duration. The SMI31-positive conglomerate inclusions (Fig. 3E) in Patients ALS1-5 and ALS1-6 were mostly TDP negative (Fig. 3F) or had only very faint staining (Fig. 3D).

G93A Mice

In normal littermates, TDP-IR was found in the neurons and some glia in the gray matter (Fig. 4A); the white matter was negative for TDP. In G1L mice, the nuclei of neurons and reactive astrocytes were stained for TDP. The

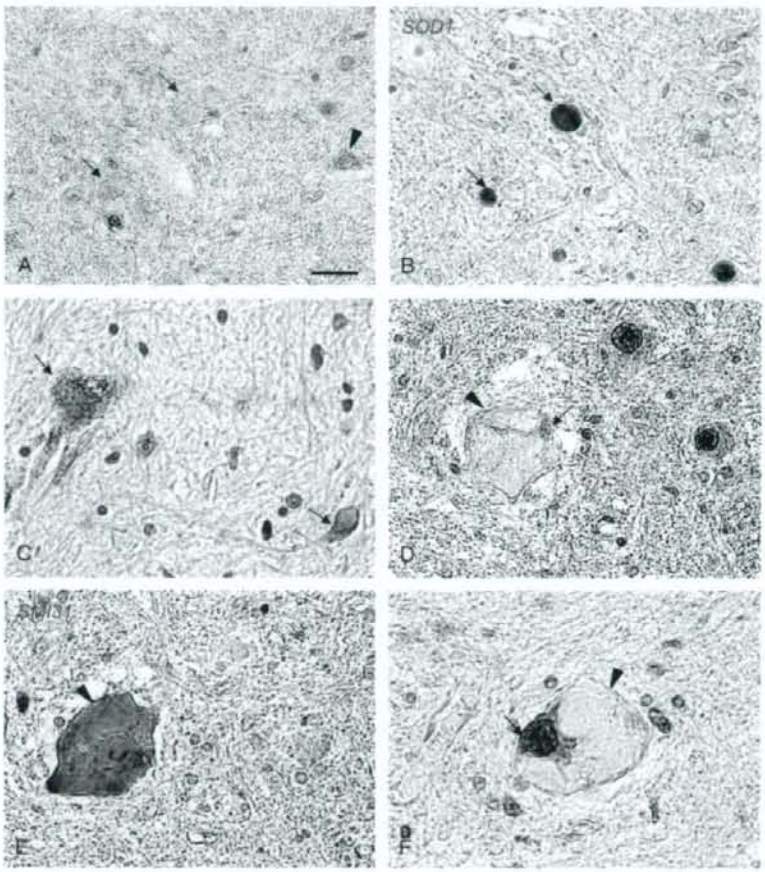

FIGURE 3. TAR DNA binding protein (TDP) staining patterns in the other amyotrophic lateral sclerosis 1 patients. **(A, B)** Superoxide dismutase 1 (SOD1)–positive Lewy body–like hyaline inclusions **(B)** are weakly stained (left, arrow) and very faintly stained (right, arrow) for TDP **(A)**. There is mislocalization in a small neuron (arrowhead) in **(A)**. **(C)** The neuron cytoplasm is diffusely stained for TDP (arrows). **(D, E)** A conglomerate inclusion is positive for SMI31 (**[E]** arrowhead) and is negative for TDP (**[D]** arrowhead). The nucleus (**[D]** arrow) is atrophic and deformed. **(F)** The TDP-positive nucleus (arrow) in a neuron containing a TDP-negative conglomerate inclusion (arrowhead) appears round and intact. Immunohistochemistry: **(A, C, D, F)** = TDP; **(B)** = SOD1; **(E)** = phosphorylated neurofilament (SMI31). **(B)** and **(E)** are serial sections of **(A)** and **(D)**, respectively. Scale bar = 20 μm.

cytoplasm of a few anterior horn cells showed a punctate TDP staining pattern, but most of the neuron nuclei were TDP positive (Figs. 4E, 5C). Neurons with TDP-negative nuclei and TDP-positive cytoplasm were rare (Fig. 4B). The TDP-positive inclusions and neurites were numerous (Figs. 4C, 5A–D), and the nuclear TDP-IR of these cells was weak (Fig. 5A). Some vacuoles were also stained for TDP (Fig. 4C). Colocalization of TDP and SOD1 was also detected in LBHIs in serial sections (Figs. 4C, D). Nuclear TDP-IR varied widely from mouse to mouse (Stages 1–4, Figs. 5A–D). In G1L mice showing a rapid clinical course and prominent LBHI-formation, nuclear TDP-IR was weak (Stage 1, Figs. 5A, E), whereas G1L mice showing a slow clinical course and less LBHI formation had strong nuclear TDP-IR (Stage 4, Figs. 5D, F). In Stage 4 mice, most of the nuclei were strongly positive and circular, but some weakly stained nuclei were atrophic or deformed (Fig. 4E). In G1H mice with a rapid disease course, TDP-IR of the neurons was weak, and nearly all LBHIs in the lumbar spinal cord were negative for TDP (Fig. 4F).

Statistical Analysis

The numbers of TDP-positive inclusions in neurons and glia were significantly lower in SALS patients with a

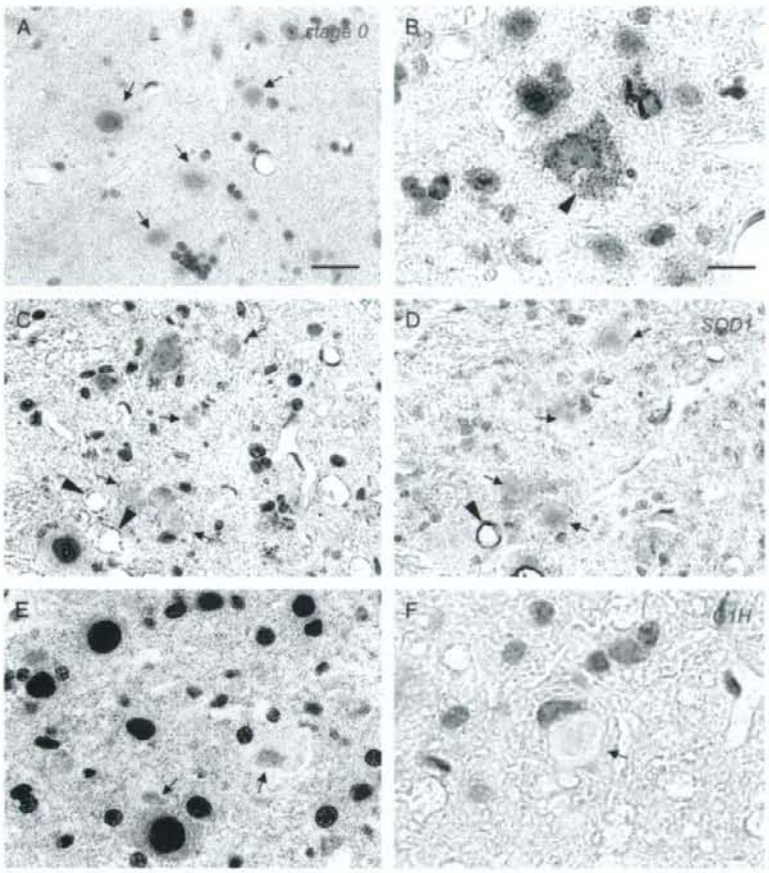

FIGURE 4. TAR DNA binding protein (TDP) pathology in G93A mice. **(A)** Nuclei in large neurons in a normal littermate (arrows) are TDP positive; their nucleoli are not stained. **(B–E)** G1L mice. **(B)** A degenerated neuron containing small vacuoles (arrowhead) in the cytoplasm has a TDP-negative nucleus and TDP-positive cytoplasm. **(C, D)** There are numerous Lewy body-like hyaline inclusions (LBHIs) that are TDP positive **(C)** and superoxide dismutase 1 (SOD1) **(D)** (arrows). Some vacuoles that are SOD1 positive **(D)** are partly stained for TDP (**C**, arrowheads). **(E)** Most of the nuclei in the neurons are strongly positive for TDP. A few nuclei that are stained only weakly (arrows) are atrophic and deformed. **(F)** The LBHI in the lumbar cord of the G1H mouse stains extremely faintly for TDP (arrow). **(A)** Normal littermate (Stage 0), **(B–E)** G1L mice, **(B–D)** Stage 3, **(E)** Stage 4, **(F)** G1H mouse. Immunohistochemistry for TDP **(A–C, E, F)** and SOD1 **(D)**. **(D)** is a serial section of **(C)**. Scale bars = (**A, C–E**) 50 μm; **(B, F)** 20 μm.

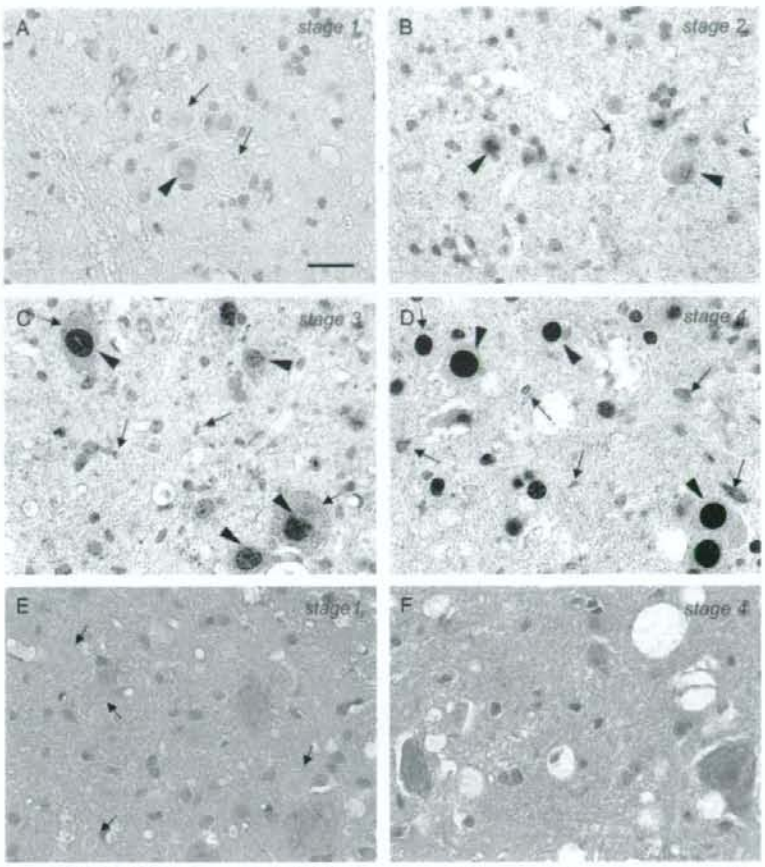

FIGURE 5. Four stages of TAR DNA binding protein (TDP) immunoreactivity in spinal cord neuron nuclei of G1L mice. **(A)** In Stage 1, nuclear immunoreactivity (arrowhead) is weak. Lewy body-like hyaline inclusions (LBHIs) (arrows) are only faintly stained or negative. **(B)** In Stage 2, nuclear immunoreactivity of neuron nuclei (arrowheads) is similar to that of normal littermates (Fig. 4A). Neurites or tiny vacuoles (arrow) also show immunoreactivity. **(C)** Immunoreactivity in Stage 3 in most of the nuclei (arrowheads) is stronger than in the normal control, but less than in Stage 4. There is diffuse and punctate cytoplasm staining and immunoreactivity in neurites (arrows). **(D)** Nuclear immunoreactivity in Stage 4 is very strong (arrowheads), and there are numerous TDP-positive neurites (arrows). **(E)** Prominent LBHIs (arrows) are evident in a Stage 1 mouse. **(F)** In a Stage 4 mouse, there are many vacuoles detected, but there is no LBHI formation. Immunohistochemistry for TDP (**A**–**D**); hematoxylin and eosin stain (**E, F**). Scale bar = 50 μm.

slow course than in those with a rapid course (Wilcoxon rank sum test: neuronal inclusions, $p = 0.0002$; glial inclusions, $p = 0.0002$). The numbers of large neurons (>37 μm) were also lower in SALS patients with a slow course than in those with a rapid course, although the level of significance ($p = 0.0264$) was lower than that for TDP-positive inclusions. The relationships among the numbers of large neurons, and TDP-positive inclusions in neurons and glia were not significant in SALS patients as a whole (Spearman correlation coefficient with 95% CI).

In G1L mice, the TDP-IR stage was positively correlated with life span (Spearman correlation coefficient with 95% CI, $r = 0.77$; 95% CI, 0.22–0.95) and negatively correlated with the formation of LBHIs ($r = -0.87$; 95% CI, −0.97 to −0.47). The correlation between life span and the number of LBHIs was also high ($r = -0.64$; 95% CI, −0.92 to 0.04). A cumulative probability plot of age at the end stage (Fig. 6) showed a higher value for the group with strong TDP-IR (Stages 3 and 4) than for those with weak TDP-IR (Stages 1 and 2); age at the end stage in the strong TDP-IR group was significantly greater than that in the weak TDP-IR group (Kolmogorov-Smirnov test, $p = 0.015$).

DISCUSSION

The TDP mislocalization from the nucleus to the cytoplasm was previously considered to be a disease-specific

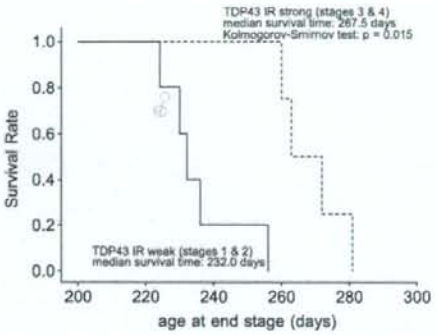

FIGURE 6. Kolmogorov-Smirnov test of the weak TAR DNA binding protein immunoreactivity (TDP-IR) groups (Stages 1 and 2) and strong TDP-IR groups (Stages 3 and 4) of G1L mice. Age at end stage in the TDP-IR strong group was significantly greater than that in the TDP-IR weak group ($p = 0.015$).

change not present in ALS1. Here, we analyzed TDP pathology in SALS and ALS1 patients and in ALS1 model mice. Our data suggest that the level of expression of TDP in the nucleus is associated with the clinical course and neurodegenerative changes in SALS patients and in ALS1 model mice.

Our observation that diffuse staining pattern was frequently observed in the cytoplasm of large neurons in SALS patients with rapid clinical courses showing mild neuronal loss suggests that TDP mislocalization starts gradually in the early phase of neurodegeneration. Most of the TDP-positive inclusions were found in atrophic neurons and glia, suggesting that the inclusions appeared later. Because no extracellular TDP-positive inclusions were apparent, neuronal TDP-positive inclusions likely disappear along with the death of the neurons.

In contrast, in SALS patients with slow clinical courses, no neurons with a diffuse TDP staining pattern in the cytoplasm were found, and TDP-positive inclusions in both neurons and glia were significantly less frequently found. Because relationships among the numbers of large neurons, those of TDP-positive inclusions in neurons, and those of TDP-positive inclusions in glia were not significant, the rarity of TDP pathology in SALS patients with a slow clinical course might not necessarily have resulted from severe neurodegeneration. The TDP pathology might be associated with a rapid clinical course in SALS. The influence of TDP-43 on the disease would then be less marked in SALS patients with a slow clinical course than in those with a rapid clinical course.

Previous studies have shown that LBHIs are not stained for TDP in ALS1 patients (16, 17, 26) and G1H mice (26).

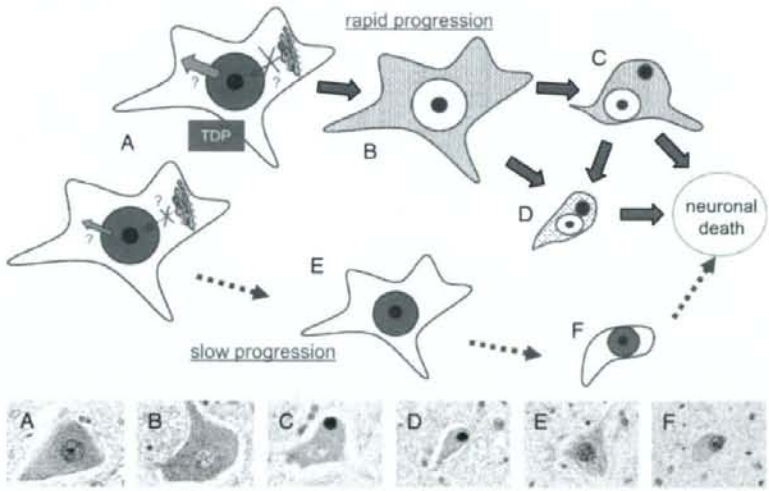

FIGURE 7. Hypothetical course of neuronal degeneration associated with changes in nuclear TAR DNA binding protein (TDP) expression in sporadic amyotrophic lateral sclerosis (SALS). **(A)** A morphologically normal neuron is subjected to an insult associated with a disturbance of TDP nuclear trafficking. The upper neuron diagrammed, from a patient with SALS, showing a rapid clinical course has marked disturbance of TDP nuclear trafficking, whereas the lower diagrammed neuron from a patient with SALS showing a slow clinical course, is only mildly affected. **(B–D)** Images show degenerating neurons at the time of rapid disease progression. **(B)** Early occurrence of TDP redistribution, i.e. low expression in nuclei and high expression in cytoplasm. **(C)** Later occurrence of cytoplasmic TDP aggregate in an atrophic neuron. **(D)** Similar aggregate of cytoplasmic TDP in a more degenerative neuron than that in **(C)**. **(E, F)** Images represent degenerative neurons at the time of slow disease progression. **(E)** Preservation of a high level of TDP expression in the nucleus of an atrophic neuron. **(F)** Successive maintenance of a high level of TDP expression in the nucleus of a more degenerative neuron. The lower 6 photographs are from SALS patients showing a rapid clinical course **(A–D)** and a slow course **(E, F)**, which correspond to the diagrammatic illustrations for each letter.

On the other hand, mislocalization of TDP to the cytoplasm in ALS1 cases (A4T, I113T) has been reported by Robertson et al (26). In the present study, TDP-positive LBHIs were clearly demonstrated in 1 ALS1 patient showing a slow disease progression, and in G1L mice, which also show slower disease progression than G1H mice. The ALS1 patients with TDP-negative LBHIs reported by Tan et al (17) showed very rapid progression within less than 1 year, and another ALS1 patient with TDP-negative LBHIs reported by Robertson et al (26) also showed rapid progression within 2 years. The difference in TDP immunoreactivity of LBHIs among ALS1 cases or between the 2 kinds of G93A mice might be a result of the difference in the clinical course or speed of SOD1 aggregation (34). The difference in morphology between TDP-positive inclusions in ALS1-1 and G1L mice and those in SALS patients would be caused by trapping of TDP-43 by SOD1 aggregation or LBHIs. The colocalization of TDP and SOD1 in LBHIs also suggests a biological relationship between SOD1 and TDP, although the specifics of that relationship are unclear.

Ayala et al (11) reported that loss of TDP in vitro results in nuclear dysmorphism, misregulation of the cell cycle, and apoptosis. Because the TDP-IR stage was positively correlated with life span in G1L mice, nuclei with low TDP-IR were atrophic and deformed in G1L mice and ALS1 patients, and an absence of TDP in the nucleus (such as that occurring through mislocalization) was frequently observed in SALS patients with a rapid clinical course, a high level of expression of nuclear TDP may play a protective role in neurons exposed to various insults. Because TDP-IR in the nucleus was inversely correlated with LBHI formation in G1L mice, TDP might have a suppressive effect on LBHI formation or toxic aggregation of SOD1, possibly through changes in the transcription and splicing of unknown genes (7, 8).

We hypothesized that rapid disease progression resulting from some insult to neurons might lead to disturbance of TDP nuclear trafficking (Fig. 7A) (35). Redistribution of TDP, with a low level of expression in the nucleus and a high level in the cytoplasm (Fig. 7B), occurs first, and cytoplasmic TDP later forms aggregates in the atrophic neurons (Figs. 7C, D). In contrast, neurons that succeed in maintaining a high level of expression of nuclear TDP (36) because of a slow shift of TDP (Fig. 7A, lower) show rather slower degeneration, and the disease progresses more slowly (Figs. 7E, F). It will be important to investigate the mechanism responsible for regulating the nuclear expression level of TDP, as this might yield a new strategy for treating not only ALS, but also other neurodegenerative disorders, including frontotemporal lobar degeneration.

ACKNOWLEDGMENTS

The authors thank T. Hamasaki and T. Sugimoto for their expert assistance with statistical analyses, and R. Yasui for technical assistance.

REFERENCES

1. Deng H-X, Hentati A, Tainer JA, et al. Amyotrophic lateral sclerosis and structural defects in Cu/Zn superoxide dismutase. Science 1993;261:1047–51
2. Rosen DR, Siddique T, Patterson D, et al. Mutations in Cu/Zn superoxide dismutase gene are associated with familial amyotrophic lateral sclerosis. Nature 1993;362:59–62
3. Kato S. Amyotrophic lateral sclerosis models and human neuropathology: Similarities and differences. Acta Neuropathol 2008;115:97–114
4. Hadano S, Hand CK, Osuga H, et al. A gene encoding a putative GTPase regulator is mutated in familial amyotrophic lateral sclerosis 2. Nat Genet 2001;29:166–73
5. Yang Y, Hentati A, Deng HX, et al. The gene encoding alsin, a protein with three guanine-nucleotide exchange factor domains, is mutated in a form of recessive amyotrophic lateral sclerosis. Nat Genet 2001;29:160–65
6. Buratti E, Brindisi A, Giombi M, et al. TDP-43 binds heterogenous nuclear ribonucleoprotein A/B through its C-terminal tail. J Biol Chem 2005;280:37572–84
7. Ayala YM, Pantano S, D'Ambrogio A, et al. Human, *Drosophila*, and *C. elegans* TDP43: Nucleic acid binding properties and splicing regulatory function. J Mol Biol 2005;348:575–88
8. Wang HY, Wang IF, Bose J, Shen CKJ. Structural diversity and functional implications of the eukaryotic *TDP* gene family. Genomics 2004;83:130–39
9. Buratti E, Baralle FE. Characterization and functional implications of the RNA binding properties of nuclear factor TDP-43, a novel splicing regulator of CFTR exon9. J Biol Chem 2001;276:36337–43
10. Mercado PA, Ayala YM, Romano M, et al. Depletion of TDP43 overrides the need for exonic and intronic splicing enhancers in the human apoA-II gene. Nucleic Acids Res 2005;33:6000–10
11. Ayala YM, Misteli T, Baralle FE. TDP-43 regulates retinoblastoma protein phosphorylation through the repression of cyclin-dependent kinase 6 expression. Proc Natl Acad Sci U S A 2008;105:3785–89
12. Kato S, Takikawa M, Nakashima K, et al. New consensus research on neuropathological aspects of familial amyotrophic lateral sclerosis with superoxide dismutase 1 (SOD1) gene mutations: Inclusions containing SOD1 in neurons and astrocytes. Amyotroph Lateral Scler Other Motor Neuron Disord 2000;1:163–84
13. Arai T, Hasegawa M, Akiyama H, et al. TDP-43 is a component of ubiquitin-positive tau-negative inclusions in frontotemporal lobar degeneration and amyotrophic lateral sclerosis. Biochem Biophys Res Commun 2006;351:602–11
14. Neumann M, Sampathu DM, Kwong LK, et al. Ubiquitinated TDP-43 in frontotemporal lobar degeneration and amyotrophic lateral sclerosis. Science 2006;314:130–33
15. Dickson DW, Josephs KA, Amador-Ortiz C. TDP-43 in differential diagnosis of motor neuron disorders. Acta Neuropathol 2007;114:71–79
16. Mackenzie IRA, Bigio EH, Ince PG, et al. Pathological TDP-43 distinguishes sporadic amyotrophic lateral sclerosis from amyotrophic lateral sclerosis with SOD1 mutations. Ann Neurol 2007;61:427–34
17. Tan C-F, Eguchi H, Tagawa A, et al. TDP-43 immunoreactivity in neuronal inclusions in familial amyotrophic lateral sclerosis with or without *SOD1* gene mutation. Acta Neuropathol 2007;113:535–42
18. Gitcho MA, Baloh RH, Chakraverty S, et al. TDP-43 A315T mutation in familial motor neuron disease. Ann Neurol 2008;63:535–38
19. Sreedharan J, Blair IP, Tripathi VB, et al. TDP-43 mutations in familial and sporadic amyotrophic lateral sclerosis. Science 2008;319:1668–72
20. Cairns NJ, Neumann M, Bigio EH, et al. TDP-43 in familial and sporadic frontotemporal lobar degeneration with ubiquitin inclusions. Am J Pathol 2007;171:227–40
21. Amador-Ortiz C, Lin W-L, Ahmed Z, et al. TDP-43 immunoreactivity in hippocampal sclerosis and Alzheimer's disease. Ann Neurol 2007;6:435–45
22. Nakashima-Yasuda H, Uryu K, Robinson J, et al. Co-morbidity of TDP-43 proteinopathy in Lewy body–related diseases. Acta Neuropathol 2007;114:221–29
23. Freeman SH, Spires-Jones TDP, Hyman BT, et al. TAR-DNA binding protein 43 in Pick disease. J Neuropathol Exp Neurol 2008;67:62–67
24. Lee EB, Lee M-Y, Trojanowski JQ, Neumann M. TDP-43 immunoreactivity in anoxic, ischemic and neoplastic lesions of the central nervous system. Acta Neuropathol 2007;115:305–11
25. Sanelli T, Xiao S, Horne P, et al. Evidence that TDP-43 is not the major ubiquitinated target within the pathological inclusions of amyotrophic lateral sclerosis. J Neuropathol Exp Neurol 2007;66:1147–53

26. Robertson J, Sanelli T, Xiao S, et al. Lack of TDP-43 abnormalities in mutant SOD1 transgenic mice shows disparity with ALS. Neurosci Lett 2007;420:128–32
27. Dal Canto MC, Gurney ME. A low expressor line of transgenic mice carrying a mutant *SOD1* gene develops pathological changes that most closely resemble those in human amyotrophic lateral sclerosis. Acta Neuropathol 1997;93:537–50
28. Parent A, Carpenter MB. *Carpenter's Human Neuroanatomy, 9th ed.* Philadelphia, PA: Lippincott, Williams &Wilkins, 1996
29. Sumi H, Nagano S, Fujimura H, et al. Inverse correlation between the formation of mitochondria-derived vacuoles and Lewy body–like hyaline inclusions in G93A superoxide dismutase–transgenic mice. Acta Neuropathol 2006;112:52–63
30. Kategawa J, Fujimura H, Ogawa Y, et al. A clinicopathological study of familial amyotrophic lateral sclerosis associated with two pair deletion in the copper/zinc superoxide dismutase (SOD1) gene. Acta Neuropathol (Berl) 1997;94:617–22
31. Kato S, Shimoda M, Watanabe Y, et al. Familial amyotrophic lateral sclerosis with a two base pair deletion in superoxide dismutase 1 (SOD1): Gene multisystem degeneration with intracytoplasmic hyaline inclusions in astrocytes. J Neuropathol Exp Neurol 1996;55:1089–101
32. Inoue K, Fujimura H, Ogawa Y, et al. Familial amyotrophic lateral sclerosis with a point mutation (G37R) of the superoxide dismutase 1 gene: A clinicopathological study. Amyotroph Lateral Scler Other Motor Neuron Disord 2002;3:244–47
33. Inoue K, Fujimura H, Toyooka K, et al. Familial amyotrophic sclerosis with L126S mutation of Cu/Zn superoxide dismutase gene. Pathological study of two cases [Abstract]. J Neurol 2006;235:120
34. Sato T, Nakanishi T, Yamamoto Y, et al. Rapid disease progression is correlated with instability of mutant SOD1 in familial ALS. Neurology 2006;65:1954–57
35. Winton MJ, Igaz LM, Wong MM, et al. Disturbance of nuclear and cytoplasmic Tar DNA binding protein (TDP-43) induces disease-like redistribution, sequestration and aggregate formation. J Biol Chem 2008; 283:13302–9
36. Wang IF, Chang HY, James Shen CK. TDP-43, the signature protein of FTLD-U, is a neuronal activity-responsive factor. J Neurochem 2008; 105:797–806

ALS 1 の神経病理と発症機序

加藤 信介

はじめに

筋萎縮性側索硬化症(amyotrophic lateral sclerosis：ALS)は，錐体路を構成する上位および下位の motor neuron を系統的に障害し，進行性筋萎縮を主症状とする原因不明の疾患である．家族性筋萎縮性側索硬化症(familial amyotrophic lateral sclerosis：FALS)は，本邦では ALS 症例の約 3.5～3.9%(欧米では約 5～10%)に存在する．この FALS のうち ALS 1 とは，Cu/Zn-superoxide dismutase (SOD 1)の遺伝子異常を伴う FALS で，常染色体優性遺伝形式をとり，FALS の約 20%に相当する[1]．

ALS 1 の神経病理

1．ALS 1 の上位および下位 motor neuron 病変

ALS 1 の上位 motor neuron の病変は SALS に比べて一般的にごく軽度であることが特徴である[1,2]．ただし，長期生存例においては上位 motor neuron の障害も顕著化してくる．ALS 1 の病変の主体は下位 motor neuron 系である[1,2]．動眼・滑車・外転の各神経核と Onuf 核以外の脳神経運動核と脊髄前角運動細胞(α-motoneuron)が変性し，消失する．脊髄前角運動細胞が変性・脱落すれば，反応性 astrocyte の増殖とともに，前角・前根が萎縮し前角内有髄線維は減少する．

2．ALS 1 の細胞病理の特徴

ALS 1 の病理像は，下位 motor neuron 病変に加えて，① 後索中間根帯の変性，② Clarke 柱 neuron と脊髄小脳路(Clarke 柱 neuron の軸索路)の変性，③ 神経細胞内 Lewy 小体様硝子様封入体(neuronal Lewy-body-like hyaline inclusion：LBHI)とアストロサイト内硝子様封入体(astrocytic hyaline inclusion：Ast-HI)の存在が特徴である[1,2]．① 腰髄では薄束，頸髄では楔状束(いわゆる Flechsig の中間根帯)が淡明化する．病変が高度になると後索中央部全体が変性を呈することもある．② Clarke 柱 neuron の変性脱落に伴い，これら neuron の軸索路である後脊髄小脳路の変性をおこす．高度になると前脊髄小脳路も侵される．

3．Neuronal LBHI と Ast-HI の特徴

Neuronal LBHI と Ast-HI については，1967 年に Hirano らにより neuronal LBHI が，1996 年に著者らにより Ast-HI が，ALS 1 の特徴的所見として記載された[1,2]．Neuronal LBHI は光顕的にヘマトキシリン・エオジン(HE)染色で eosinophilic core と淡い halo よりなり，あたかもパーキンソン病の Lewy 小体のように見えるところにその名の由来がある(図 1 A)．光顕上内部は無構造で均一であるため hyaline という表現がなされている．Ast-HI については，HE 染色では neuronal LBHI とほぼ同一構造を呈し，eosinophilic で均質無構造な hyaline 様を呈している．多くは円形から楕円形であり(図 2)，時に eosinophilic core と淡い halo を認めることがある．

Neuronal LBHI と Ast-HI はともに免疫組織化学的に SOD 1 に強陽性を示す(図 1 B)[1,2]．特徴的なことは，両者は野生型と変異型の両者の SOD 1 epitope を有していることである[2]．超微形態的には，neuronal LBHI も Ast-HI もともに約 15～25 nm 径の granule-coated fibril と顆粒状構造物(granular material)からなっている(図 3，4)．この granule-coated fibril の横断面は管状構造をなしておらず，顆粒稠密状を呈している．その形成過程については，granular material が linear 状に凝集し，granule-coated fibril が形成されてくる超微形態学的形成像がとらえられている[2]．変異 SOD 1 を core protein の一つとして凝集し，野生型 SOD 1 をも取り込みながら，granule-coated fibril が形成されるものと著者は考えている．

4．ALS 1 と Bunina body

細胞病理学上 ALS 1 のもう一つの特徴は，Bunina body が観察されないことである[1,2]．このことは，ロシアの女

かとう しんすけ　鳥取大学医学部附属脳幹性疾患研究施設准教授/脳神経病理部門

0289-0585/08/¥500/論文/JCLS

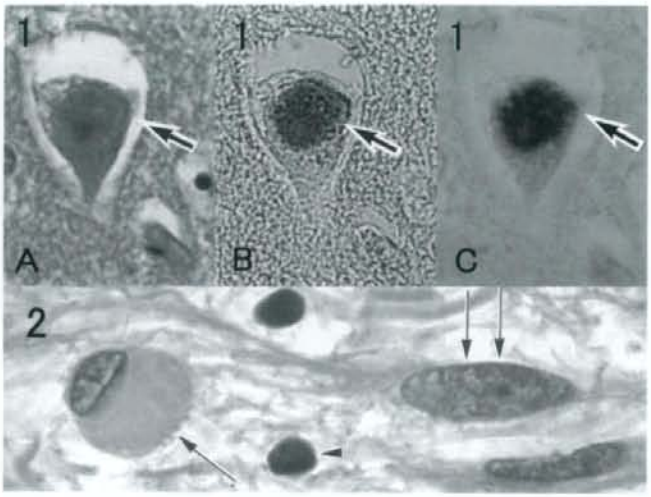

図 1，2　LBHI と Ast-HI の光顕像

図 1　A）LBHI（矢印）の HE 染色．B）LBHI の SOD 1 免疫染色．C）LBHI の CML（N^{ε}-carboxymethyl lysine）免疫染色．LBHI の core protein の一つである SOD 1 がメイラード反応を受け，細胞毒性のある AGE の一つである CML 修飾 SOD 1 を形成している（タンパク質凝集体仮説）[3]．A～C は同一切片多重免疫組織化学染色法．

図 2　Ast-HI（矢印）を有する細胞の核は oligodendroglia の核（矢頭）とは異なり，reactive astrocyte の核（二重矢印）に酷似している．HE 染色．

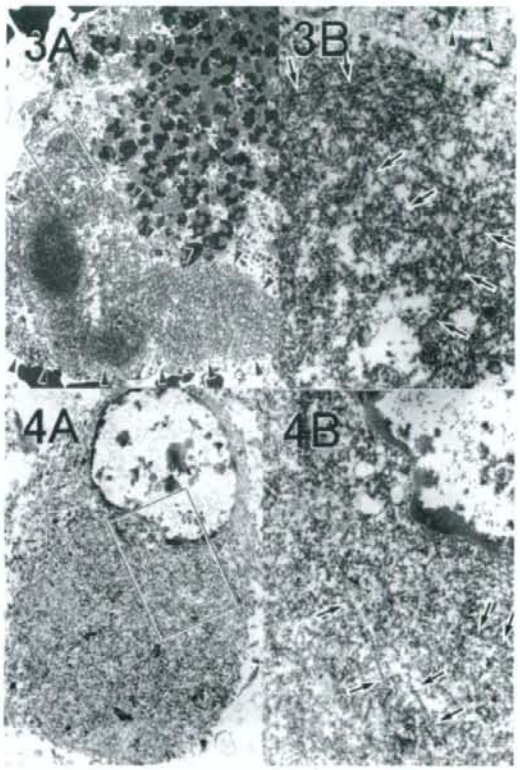

図 3，4　LBHI と Ast-HI の電顕像

図 3　A）LBHI の弱拡大像（矢頭），異常線維が密に集まっている部位が core で，粗に存在している周辺部が halo に相当する．B）LBHI（A の矩形部分）の強拡大像．LBHI の本体は約 15～25 nm 径の granule-coated fibril（矢印）であり，neurofilament（矢頭）はわずかに周辺にみられるのみである．

図 4　A）Ast-HI の弱拡大像．アストロサイトの胞体の大部分は granule-coated fibril によって占拠されてしまっている．B）Ast-HI（A の矩形部分の拡大）の強拡大像．Ast-HI の本体は LBHI と同一の約 15～25 nm 径の granule-coated fibril である（矢印）．

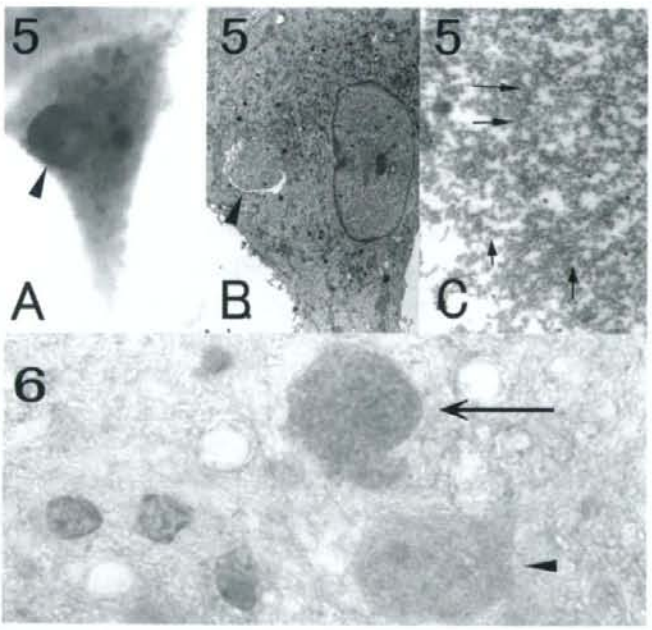

図 5，6　ALS 1 発症機序の最新知見

図 5　小胞体ストレス仮説[4]

A）Neuroblastoma の培養細胞に L 84 V-SOD 1 を過剰発現させ ER stress を加えたところ，光顕的には LBHI 様封入体が胞体内に形成されている（矢頭）．B）封入体の電顕弱拡大像（矢頭）．C）封入体の電顕強拡大像．電顕的には約 15～25 nm 径の granule-coated fibril（矢印）が形成されている．

図 6　酸化ストレス仮説[5]

酸化型 SOD 1 のみを特異的に認識する抗 OxSOD 1 抗体にて，LBHI が強陽性を示している（矢印），残存神経細胞は陰性を示している（矢頭）．

性病理学者 Bunina が報告した ALS 症例は FALS の 2 家系 2 症例である[1,2]ことを考慮すれば，興味深い特徴であると著者は考えている．おそらく，Bunina が検索した症例は，SOD 1 遺伝子異常を伴わない FALS 症例で，神経病理学的に SALS とほぼ同一の病理像を呈する FALS 症例群[2]であったのだろうと著者は想像している．蛇足になるが，SALS と同一神経病理像を有する，SOD 1 遺伝子異常を伴わない FALS では，SALS の特徴的病理学的所見である skein-like inclusion (SLI) や round hyaline inclusions (RHI) も高率に観察される[2]．もちろん Bunina body が同定されるのはいうまでもないことである．

5．I 113 T を伴う ALS 1

I 113 T 変異 SOD 1 を伴う ALS 1 は，LBHI/Ast-HI の所見を欠き，neurofilamentous conglomerate inclusion (NFCI) を高率に形成する特徴がある[1,2]．NFCI は，HE 染色ではごくわずかに好酸性を呈する均一な球状，または分葉状構造物である．免疫組織化学的には pNFP に強陽性を呈する．Ubiquitin には多くの NFCI は陰性を呈するものの，NFCI の内部の一部には ubiquitin 陽性構造物を認めることもある．超微形態的には NFCI は neurofilament の束が三次元的に糸巻き・渦巻きを形成して球状構造をしている．もちろん，NFCI は SALS(5%以下)でも観察される．

6．ALS 1 と TDP-43[2]

細胞病理学上興味ある所見として，H 48 Q と E 100 G の変異 SOD 1 を伴う ALS 1 は，SALS の特徴的病理学所見である SLI を有するということである[1,2]．最近注目を集めている TDP-43 という観点から論ずれば，SALS，変異 SOD 1 に関連しない FALS，fronto temporal lobor degeneration with motor neuron disease (FTLD-MND：terminology 上は ALS with dementia：ALSD と同一) において出現する SLI は TDP-43 陽性を呈し，ALS 1 に認められる LBHI は TDP-43 陰性である．SOD 1 遺伝子異常を伴うヒト FALS を prototype とした G 37 R，G 85 R，G 93 A transgenic mice では，TDP-43 の異常を認めない．これらの TDP-43 の所見は，変異 SOD 1 に関連しない motor neuron death には TDP-43 が関与し，一方変異 SOD 1 に関連する motor neuron death には TDP-43 が本質的には関与していないという仮説が直感的に成立しそうな感じを与える．しかし，LBHI と SLI とを一緒に有する H 48 Q と SLI を有する E 100 G の ALS 1 の存在は，この仮説の実証は容易ではないと物語っているように著者には思われる．

ALS 1 の発症機序

ALS 1 の発症機序の仮説として以下に述べる諸説があるが，実際はいくつもの要因が相互に関与している[1]と著者は考えている．

1．タンパク質凝集体仮説

ALS 1 においては，SOD 1 陽性の LBHI/Ast-HI の存在 (図 1 B) が変異 SOD 1 の "gain of function" の実体の一つである．SOD 1 は最もメイラード (グリケーション) 反応を受けやすい蛋白の一つであり，グルコースによりメイラード反応を受け，アマドリ化合物を介して糖化反応最終産物 (advanced glycation endoproduct：AGE) を形成する (図 1 C)[3]．変異 SOD 1 はよりメイラード反応を受けやすく AGE を形成しやすい[3]．AGE が不溶性で細胞毒性のある化合物であることを考慮し，メイラード反応等の様々な反応によって生じたタンパク質凝集体により細胞死を惹起するという仮説を aggregation toxicity と呼んでいる[3]．LBHI/Ast-HI が形成される際に，生存に必要不可欠な正常構成蛋白や細胞特異性蛋白をも胞体内から封入体内部に取り込むことにより，細胞死を加速させる現象も含めて aggregation toxicity とここでは広く解釈する[3]．即ち，変異 SOD 1 が細胞内に存在することで aggregation toxicity を引きおこし，細胞死を惹起させるとするタンパク質凝集体仮説は病理形態学からは極めて馴染みやすい仮説といえる．

2．小胞体 (endoplasmic reticulum) ストレス (ER stress) 仮説

変異 SOD 1 を有する細胞においては，光顕的 hallmark は LBHI/Ast-HI であり，電顕的 hallmark は 15～25 nm 径の granule-coated-fibril である[1,2]．換言すれば，15～25 nm 径の granule-coated-fibril が存在していれば，変異 SOD 1 がその細胞に存在する結果であるといえる．Neuroblastoma cell line の SK-N-SH 培養細胞に L 84 V-SOD 1 を過剰発現させ ER stress を加えたところ，光顕的には LBHI 様封入体が胞体内に形成され (図 5 A)，電顕的には 15～25 nm 径の granule-coated-fibril が形成された (図 5

B, C)という最新のYamagishiらと著者らとの共同研究結果[4]がある．この事実は，変異SOD 1の形態的hallmarkである15～25 nm径のgranule-coated-fibril形成には，ER stressがALS 1発症に強く関与していることを端的に証明している．

3．酸化ストレス仮説

Peroxynitrateを介する酸化ストレス発症機序仮説は，O_2^-は一酸化窒素(NO)に対する結合能がSOD 1に対する結合能の約3倍であるという化学反応学的根拠に基づいた仮説である．変異SOD 1が存在することにより，細胞内で生じたすべてのO_2^-が変異型と野生型のSOD 1と反応できず，一部のO_2^-がNOとの反応に傾き，細胞毒性の高いperoxynitrateやhydroxy radicalsが産生され，神経細胞死を惹起させるとする仮説である．また，変異SOD 1においては，活性中心のCuの配位結合が不安定になり，同時に，立体構造の変化によりCuの活性中心部位が開大してしまい，活性中心にあるCuが通常では反応しない基質と反応することで活性酸素を産生してしまうとする酸化ストレス仮説である．しかし，現在では両仮説に対しては，否定的な実験報告が多く，酸化ストレスがALS 1の発症に関与することはあっても，中心的な役割を果たしていないと考えられている[1]．一方，G 93 A-SOD 1 transgenic mouseの病態機序には，確かに酸化ストレスが存在しているという最新知見が発表されている．即ち，SOD 1自身が酸化されていて，その酸化型SOD 1(Cys 111-peroxide SOD 1)がLBHIに取り込まれているという事実(図6)がFujiwaraら[5]より報告されている．この事実は，G 93 A-SOD 1 transgenic mouseの発症に中心的役割をしているSOD 1自身に酸化ストレスが確かに加わっていることを見事に説明している．

4．ミトコンドリア仮説

G 93 A-SOD 1 transgenic mouseの基本病理学像は，motor neuron death，LBHI/Ast-HIの出現(inclusion pathology)，vacuolation pathologyの3つである[2]．このvacuolation pathologyの主病巣がミトコンドリアであるという病理形態学的事実は，ミトコンドリア仮説を強く支持する．野生型と変異型の両方のSOD 1は主に細胞質に存在すると同時にミトコンドリアの膜間領域にも存在している．従って，膜間領域に変異SOD 1が存在するために，最終的にapoptosisを引きおこすという仮説が提唱されている[1]．ミトコンドリア仮説は，G 93 A-SOD 1 transgenic mouseにおけるミトコンドリア由来と考えられているvacuoleが，病態の中心的役割をなすG 93 A変異SOD 1に強く染色されるという免疫組織化学的事実にも強く裏打ちされている[2]．ただし，ヒトALS 1の病理像にはvacuolation pathologyは基本的には存在しない[2]．

5．興奮性アミノ酸仮説

ALS 1においても興奮性アミノ酸仮説が提唱されている．詳細については孤発性ALSの発症機序の項を参照して頂きたい．

6．その他

ALS 1のその他の発症機序の詳細については，著者らの成書[1]に記載してあるので参照して頂きたい．

謝辞：　本研究の一部は，文部科学省科学研究費補助金，基盤研究(C)：17500229(SK)と厚生労働科学研究費補助金こころの健康科学研究事業：H 18-こころ-一般-025(SK)および厚生労働科学研究費補助金難治性疾患克服対策研究事業：H 17-難治-一般-044(SK)の助成により行った．

文　献

1) Kato S, Shaw P, Wood-Allum C, et al. Amyotrophic lateral sclerosis. In：Dickson D, editor. Neurodegeneration：the molecular pathology of dementia and movement disorders. Basel：ISN Neuropath Press：2003. p. 350-68.
2) Kato S. Amyotrophic lateral sclerosis models and human neuropathology：similarities and differences. Acta Neuropathol.：Online Publish 2007, Nov, DOI10. 1007/s00401-007-0308-4.
3) Kato S, Horiuchi S, Liu J, et al. Advanced glycation endproduct-modified superoxide dismutase-1 (SOD 1)-positive inclusions are common to familial amyotrophic lateral sclerosis patients with SOD 1 gene mutations and transgenic mice expressing human SOD 1 with a G 85 R mutation. Acta Neuropathol. 2000；100：490-505.
4) Yamagishi S, Koyama Y, Katayama T, et al. An in vitro model for Lewy body-like hyaline inclusion/astrocytic hyaline inclusion：induction by ER stress with an ALS-linked SOD 1 mutation. PLoS One. 2007；2：e 1030.
5) Fujiwara N, Nakano M, Kato S, et al. Oxidative modification to cysteine sulfonic acid of cys 111 in human copper-zinc superoxide dismutase. J Biol Chem.：Online Publish 2007, Oct3.

Journal of Neuroscience Research 86:2512–2523 (2008)

Accumulation of Chondroitin Sulfate Proteoglycans in the Microenvironment of Spinal Motor Neurons in Amyotrophic Lateral Sclerosis Transgenic Rats

Hideki Mizuno, Hitoshi Warita,* Masashi Aoki, and Yasuto Itoyama

Division of Neurology, Department of Neuroscience, Tohoku University Graduate School of Medicine and Tohoku University Hospital ALS Center, Sendai, Japan

Chondroitin sulfate proteoglycans (CSPGs) are the major components of extracellular matrix in the central nervous system. In the spinal cord under various types of injury, reactive gliosis emerges in the lesion accompanied by CSPG up-regulation. Several types of CSPG core proteins and their side chains have been shown to inhibit axonal regeneration in vitro and in vivo. In the present study, we examined spatiotemporal expression of CSPGs in the spinal cord of transgenic (Tg) rats with His46Arg mutation in the *Cu/Zn superoxide dismutase* gene, a model of amyotrophic lateral sclerosis (ALS). Immunofluorescence disclosed a significant up-regulation of neurocan, versican, and phosphacan in the ventral spinal cord of Tg rats compared with age-matched controls. Notably, Tg rats showed progressive and prominent accumulation of neurocan even at the presymptomatic stage. Immunoblotting confirmed the distinct increase in the levels of both the full-length neurocan and their fragment isoforms. On the other hand, the up-regulation of versican and phosphacan peaked at the early symptomatic stage, followed by diminishment at the late symptomatic stage. In addition, double immunofluorescence revealed a colocalization between reactive astrocytes and immunoreactivities for neurocan and phosphacan, especially around residual large ventral horn neurons. Thus, reactive astrocytes are suggested to be participants in the CSPG accumulation. Although the possible neuroprotective involvement of CSPG remains to be investigated, the present results suggest that both the reactive astrocytes and the differential accumulation of CSPGs may create a nonpermissive microenvironment for neural regeneration in neurodegenerative diseases such as ALS.

Key words: amyotrophic lateral sclerosis; chondroitin sulfate proteoglycan; microenvironment; SOD1; transgenic rat

Amyotrophic lateral sclerosis (ALS) is a relentless and progressive neurodegenerative disease characterized by adult-onset selective loss of motor neurons, which causes skeletal muscle atrophy and weakness, and ultimately death. In approximately 10% of all ALS patients, this condition is familial, mainly with inheritance of an autosomal dominant trait (Haverkamp et al., 1995). Despite clinical and genetic heterogeneity, the pathologies of familial ALS and that of sporadic ALS are similar, suggesting a common pathomechanism. In about 20% of familial ALS families, this disease is linked to mutations in the *Cu/Zn superoxide dismutase* (*SOD1*) gene (Aoki et al., 1993; Rosen et al., 1993). Several lines of transgenic (Tg) rodents ubiquitously overexpressing a mutant *SOD1* transgene recapitulate the ALS phenotype (Gurney et al., 1994; Nagai et al., 2001), whereas *SOD1* knockout mice do not develop motor neuron degeneration (Reaume et al., 1996), indicating a gain of toxicity of mutant SOD1. However, the precise mechanisms of motor neuron death remain to be elucidated (Boillee et al., 2006a).

Recent data from wild-type/mutant SOD1 chimeric mice (Clement et al., 2003) and mice carrying a deletable mutant *SOD1* gene in a cell type-selective manner (Boillee et al., 2006b) demonstrated the noncell-autonomous toxicity of mutant SOD1. These studies have highlighted the involvement of nonneuronal cells, suggesting the significance of the microenvironment surrounding motor neurons. Although no cell-restorative therapy for ALS has been established to date, the possibility of replacing neuronal or nonneuronal cells is of growing interest. Among nonneuronal cells, glial cells constitute the largest cell population in the adult central

Contract grant sponsor: Japanese Ministry of Health, Labor and Welfare; Contract grant number: B: 18790586; Contract grant number: C: 19590977; Contract grant number: 18A-8; Contract grant sponsor: Haruki ALS Research Foundation (to H.W., M.A., Y.I.).

*Correspondence to: Hitoshi Warita, MD, PhD, 1-1 Seiryo-machi, Aoba-ku, Sendai 980-8574, Japan.
E-mail: als@em.neurol.med.tohoku.ac.jp

Received 4 September 2007; Revised 20 December 2007; Accepted 30 January 2008

Published online 25 April 2008 in Wiley InterScience (www.interscience.wiley.com). DOI: 10.1002/jnr.21702

nervous system (CNS). Furthermore, glial cell hypertrophy, proliferation, and accumulation in the affected region are prominent features in CNS damage, including ALS. These glial responses under disease conditions are referred to as *reactive gliosis*, which leads to glial scar formation (Silver and Miller, 2004).

Reactive gliosis is usually accompanied by up-regulation of the regeneration-inhibitory molecules in the extracellular matrix (ECM). This process is believed to create a nonpermissive microenvironment for regeneration. Among the inhibitory molecules, chondroitin sulfate proteoglycans (CSPGs) are the major components in the ECM. Previous reports have demonstrated that CSPGs are inhibitory to neurite outgrowth in vitro and are up-regulated and accumulated after various types of CNS injury in vivo. However, under chronic disease conditions such as neurodegeneration, the expression and distribution of CSPGs have not been investigated previously, except for a few earlier reports (DeWitt et al., 1993, 1994).

The glial role in ALS pathophysiology remains controversial (Neusch et al., 2007), however, the reactive gliosis in the spinal cord has already been reported as a pathological event. Although previous studies have suggested the presence of neural stem/progenitor cells in the intact spinal cord (Gage, 2000; Horner et al., 2000), recent reports have provided controversial results on spontaneous neurogenesis and insufficient evidence for intrinsic regeneration in the spinal cord of mutant *SOD1* Tg mice (Warita et al., 2001; Chi et al., 2006; Liu and Martin, 2006; Guan et al., 2007). These previous studies suggest an absence of inter-/intracellular signals and an inappropriate microenvironment for promoting an endogenous repair mechanism. Thus, substantial interest has recently been paid to the microenvironment, in the context of possible development of cell-restorative therapy with both cell transplantation and endogenous neural progenitor activation (Busch and Silver, 2007).

The present study, therefore, focused on CSPGs such as neurocan, versican, and phosphacan in the microenvironment surrounding degenerating motor neurons. We examined a possible change of the CSPG expression in the adult spinal cord of a rat ALS model and found a significant and differential accumulation of the CSPGs in the neurodegenerative lesion.

MATERIALS AND METHODS

Experimental Animals

Tg rats expressing ALS-associated mutation, His46Arg (H46R) in the human *SOD1* gene (Aoki et al., 1993), were used in this study. They were established in our laboratory, as was the case in our previous report (Nagai et al., 2001). The Tg rats hemizygous for H46R mutation were crossed with wild-type Sprague-Dawley (SD) rats (Slc:SD; Japan SLC, Inc., Shizuoka, Japan) to produce Tg and non-Tg offspring. The Tg progeny were genotyped by polymerase chain reaction amplification of tail DNA with specific primers for exon 4 (Nagai et al., 2001). The H46R Tg rats display an adult-onset motor neuron disease (MND) with later onset, slower progression, and less variability in the phenotype than in the case of Gly93Ala (G93A) transgenic rats (Nagai et al., 2001; Matsumoto et al., 2006). At about 24–25 weeks of age, the Tg rats develop progressive spastic paralysis beginning with a unilateral hindlimb, leading to death about 4 weeks later. The onset of clinical phenotype is delayed by approximately 4–5 weeks in the present Tg rats compared with the original H46R Tg line (Nagai et al., 2001) through multiple passage. The female H46R Tg rats were divided into three experimental groups: presymptomatic (aged 24 weeks, designated *Pre*), early symptomatic (aged 26 weeks, *ES*), and late symptomatic (aged 28 weeks, *LS*). We examined a total of 16 Tg rats and 18 age-matched non-Tg littermates as controls. The rats were housed in a specific pathogen-free animal facility and allowed access to food and water ad libitum. Throughout this study, the animals were handled in the accordance with the *Guide for the care and use of laboratory animals* specified by the Laboratory Animal Welfare Act (National Institutes of Health). All experimental protocols and procedures were approved by the Animal Committee of the Tohoku University Graduate School of Medicine.

Immunofluorescence

The rats were deeply anesthetized with diethyl ether and perfused transcardially with heparinized saline, followed by ice-cold 4% paraformaldehyde in 0.1 M phosphate buffer (PB), pH 7.4. Their lumbar spinal cords (L4–L5) were immediately removed and further fixed by immersion in the same fixative overnight at 4°C, followed by cryoprotection with a series of increasing concentration of sucrose (10% and 20% wt/vol) in 0.1 M PB at 4°C. The tissue samples were embedded in Tissue-Tek O.C.T. compound (Sakura Finetek, Tokyo, Japan) and quickly frozen in 2-methylbutane cooled with liquid nitrogen, then stored at −80°C. Ten-micrometer transverse sections of lumbar spinal cords were cut on a cryostat (CM3050; Leica Instruments, Nussloch, Germany), collected on MAS-coated glass slides (Superfrost; Matsunami Glass, Osaka, Japan), and stored at −80°C. The cryosections were washed in Tris-buffered saline (TBS), pH 7.4. Nonspecific binding was blocked with 5% normal goat serum (Vector Laboratories, Burlingame, CA) and 0.3% Triton X-100 in TBS for 30 min at room temperature (RT). After blocking, the sections were incubated with primary antibodies in the blocking solution overnight at 4°C. We employed the following primary antibodies: rabbit anti-glial fibrillary acidic protein (GFAP) polyclonal IgG (1:1,500; Dako, Glostrup, Denmark), rabbit anti-glutathione S-transferase-π (GST-π) polyclonal IgG (1:1,500; Assay Designs, Ann Arbor, MI), rabbit antineurofilament-H polyclonal IgG (1:1,000; Chemicon International, Temecula, CA), rabbit anti-ionized calcium-binding adapter molecule-1 (Iba-1) polyclonal IgG (1:1,500; Wako Pure Chemical, Osaka, Japan), mouse anti-neurocan monoclonal IgG (1:3,000; clone 650.24; Chemicon International) that is specific for the full-length neurocan core protein and also reacts with the C-terminal fragment, rabbit anti-glycosaminoglycan-α (GAGα) domain of versican V2 (a CNS-specific